Comparison of Industrial Agitation for Simulated Batch Reactor Vessel Mixing in Bioethanol Fermentation

H. Rana
Loughborough University
h.rana-11@alumni.lboro.ac.uk

Abstract

This paper presents the investigation into the phenomena during batch reactor vessel mixing comparing different agitation equipment; the Rushton turbine and the Marine propeller; in the production of bioethanol by yeast fermentation using *Saccharomyces cerevisiae*. The key factors addressed in selecting between equipment were fluid vector patterns and flow, energy dissipation resulting in shear damage to yeast cells, agitation power consumption, critical stirring velocities for cell suspension, and capital and process operating costs. These were investigated with the use of COMSOL Multiphysics, employing different Computational Fluid Dynamics (CFD) modules. Upon gaining insight into the physical phenomena within the vessel, it was found that both agitators are effective when used within the critical stirring velocity range, however, the Marine propeller was deemed a more suitable choice from a cost optimisation perspective.

Keywords: Mixing, bioethanol, fermentation, batch reactor, Rushton turbine, Marine propeller, agitation, process optimisation.

1. Introduction

Bioethanol production is an increasingly important venture within the biofuels industry, where the primary product ethanol is used nowadays as an additive to petrol or diesel in order to comply with environmental policy and energy demands. This forms part of a global attempt to reduce fossil fuel consumption and produce sustainable energy. In yeast fermentation ethanol production, a key parameter in the process is that of batch mixing, which enables reaction to occur within the fermenter but also is optimised to ensure yeast cells are not victim to shear damage, enabling the fermentation reactions to occur to their kinetic optimal point. In industrial bioethanol reacting vessels several agitators are used, however, comparison of different agitation is largely achieved on a trial and error basis. Agitation tends to be kept low to create a bio-friendly environment; however, this is not efficient from a process point of view. Producing 3D simulations of these fermentations using two widely used agitators allows for better insight into the vessel mixing phenomena, and enables comparison of the agitators selected to be made for this very specific and highly important reaction process.

2. Theory & Modelling Methods

2.1 Governing Equations

The equations governing the batch reactor mixing are presented below.

$$Re = \frac{\rho N_i {D_i}^2}{\mu} \qquad \text{Eq. 1}$$

Eq. 1 (Nienow, 2014) correlates the key process parameters to determine the Reynolds number of the vessel operation. N (s^{-1}) is the operating stirrer speed indicating agitator revolutions per second, μ (Pa.s) is the broth viscosity, D_i the impeller diameter, ρ the broth density. *Re* allows the system to be characterized as either laminar or turbulent flow. The term N_P, the dimensionless power number given by Eq. 2, is in essence the drag coefficient for the vessel mixing and relates with *Re* to indicate the flow in which the vessel operates, as shown in Appendix 8.1 Fig.4.

$$N_P = \frac{P}{\rho {N_i}^3 {D_i}^5} \qquad \text{Eq. 2}$$

The mixing time t_m, is a useful parameter to assess the effectiveness of mixing in the vessel, given in Eq. 3 (Doran, 1995). It is the time required for a given degree of homogeneity in concentration to be reached from a starting time at which the substance (feed substrate – sucrose) is introduced into the vessel. The simulation particle tracing module allows for this to be determined in greater complexity for the two agitators.

$$N_i t_m = \frac{1.54\, V_l}{{D_i}^3} \qquad \text{Eq. 3}$$

Zwietering's correlation for critical stirrer speed, presented by McCabe, et al., 2005, relates mixing and suspension factors with the agitation speed of the vessel in order to determine critical

speed, n_c, that is a minimum requirement for complete suspension of solid particles. The application of Eq. 4 to the model being developed ensures that the *S. cerevisiae* cells will be in suspension whilst in the reactor due to agitation, enabling reactions to occur suitably.

$$n_c D_i^{0.85} = S v^{0.1} D_p^{0.2} \left(g \frac{\Delta\rho}{\rho'}\right)^{0.45} B^{0.13} \quad \text{Eq. 4}$$

Further to the modelling of a suitable critical stirrer speed, an important characteristic to consider with yeast cells in a bioreactor is the potential effect of 'shear damage' on the cells caused by agitation. Eq.s 5 and 6, Kolmogorov's microscales, allow the sizes of eddy turbulences λ_k to be calculated to determine whether they are within range to rupture the cells. ε_T (W/kg) is the mean specific energy dissipation rate.

$$\lambda_k = f(\nu, \varepsilon_T) = \left(\frac{\nu^3}{\varepsilon_T}\right)^{\frac{1}{4}} \quad \text{Eq. 5}$$

$$\varepsilon_T = \frac{P}{\rho V} = \frac{P_o N_i^3 D_i^5}{V} \quad \text{Eq. 6}$$

Lastly, in modelling gas-liquid mass transfer in the aerobic fermentation vessel, the oxygen transfer rate (OTR) can be considered to equal the oxygen uptake rate (OUR) in optimized mass transfer of oxygen to yeast, and is governed by the mass transfer coefficient k_La (s^{-1}), given in Eq.s 7 and 8 (Riet, 1979).

$$OUR = k_L a \Delta C_{O_2} \quad \text{Eq. 7}$$

$$k_L a = A(\varepsilon_T)_g^{\alpha} (v_s)^{\beta} \quad \text{Eq. 8}$$

2.2 Preliminary Modelling

MATLAB ® and Polymath were used for the defining and solving of the kinetic model, given in Eq.s 9-11, developed based on Fogler's work in the field (Fogler, 2006).

$$\frac{dC_C}{dt} = k_{obs} \frac{\mu_{max} C_S C_C}{K_S + C_S} - (k_d + k_t C_t) C_C \quad \text{Eq. 9}$$

$$\frac{dC_s}{dt} = -Y_{s/c} r_g - m C_C \quad \text{Eq. 10}$$

$$\frac{dC_P}{dt} = Y_{P/C} k_{obs} \frac{\mu_{max} C_s C_C}{K_s + C_s} \quad \text{Eq. 11}$$

C_C, C_S and C_P are the concentrations of yeast cells, sucrose substrate and product, respectively. Eq.s 9-11 model the concentrations over time of all material within the reacting vessel, and were applied to the overall reaction of:

$$C_6H_{12}O_6 + 0.42O_2 + 0.91NH_3 \rightarrow 5.36CH_{1.79}O_{0.56}N_{0.17} + 2.57H_2O + 0.64CO_2$$

3. COMSOL Multiphysics

COMSOL simulations of the batch vessels were generated, with calculated inputs using Eq.s 1-11, making use of parameters and data found to be close to that used in industrial practice in order to mimic an industrial operating environment as closely as possible. The two selected commonly used industrial agitators - the Rushton turbine and the Marine propeller – were modelled in CAD (see Appendix 8.3 for example 2D) using Fig.1 ratios (Doran, 1995).

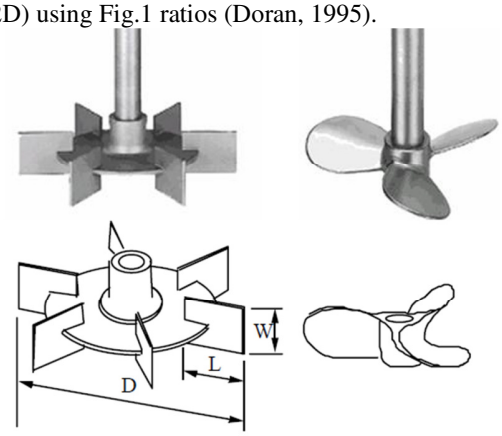

$$L = \frac{D_i}{4}, W = \frac{D_i}{5}, disc\ diameter = \frac{3D_i}{4}$$

Figure 1: Modelling ratios for the Rushton turbine (left) and Marine propeller (right).

Simulation was completed by making use of the coupling of several physics modules imported into the computational model; CFD - turbulent fluid flow; the mixing module - fluid flow with rotating machinery; and CAD import. Wall distance physics were also implemented, and dissipation of energy throughout the fluid contents of the reactor as a result of eddy currents was assessed during agitation between 0 to 2 revolutions per second. Fluid flow patterns in the vector planes *x*, *y* and *z* were examined to identify the flow vector most impactful during agitation.

For a determined *Re* of 4.2×10^5, turbulent flow functions were used throughout simulations (see Appendix 8.1 Fig.4).

4. Results & Discussion

4.1 Velocity vectors

The velocity vectors addressed in the *x*, *y* and *z* direction give an indication to the magnitude of the velocity in all 3 axes of the 3D model, generated in a 2D plane in COMSOL. Whilst they provide an indication of the flow in these axes, they are not resultants; the flow patterns are a representation of the combined velocity in all axes. Positive data values were returned by the simulation when indicating flow movement in the leftward direction for *x*-vector, flow into the screen for the *y*-vector, and upward for the *z*-vector.

Comparing the simulations for the Rushton turbine agitated vessel with the marine propeller, in the *x*-vector plane, greater velocity was observed as generated by the Rushton turbine for a given stirring speed. This would be due to the fact that Rushton turbine plates are larger in height than the impeller plates on the Marine propeller, thus the magnitude of force exerted to generate flow is greater (see Fig.1).

In the *y*-vector direction, the distributions appeared to be relatively similar. The Rushton turbine plates extend further out than the Marine propeller plates, due to their geometric design. This results in more distortion in the flow profile in the Rushton agitated vessel near the impeller.

In the *z* direction, the fluid flows towards the impellers during agitation, which shed light on the motion of flow around them. The impellers pushed the fluid away from the sides of the plates, creating vortexes that draw fluid in from underneath and above the impellers. The effect enhances mixing, and occurs to a much greater degree in the vessel agitated by the Rushton turbine.

Thus the Rushton turbine appears the effective choice in terms of vector velocity agitation at the critical stirring speed range.

4.2 Streamline flow

Streamline flow gives an indication into the flow trajectory during mixing as a result of impeller activity. This aids towards monitoring sucrose feed distribution within the vessel post-addition. Once again, the Rushton turbine was deduced as the more effective agitator, as it creates larger vortexes, hence better mixing.

4.3 Simulation limitations

The main use of the simulation has been to allow for the two impellers to be compared in the light of the different discussed physical aspects; the velocity vectors, streamline flow and quantifying the magnitude of eddy turbulences formed within the vessel and comparatively between the two agitators. Yeast rupture is the important product quality consideration to be made, as shearing damage would prevent the yeast from fermenting the sucrose to a suitable standard for ethanol production, and would further reduce profit of saleable recovered yeast. Using the turbulence lengths determined from the simulations, calculations using Eq.s 5 and 6 were completed to assess which agitator would be most harmful to vessel cells.

4.4 Turbulence dissipation & critical speed

The generation of eddy turbulences and their dissipation was found to be within the range of 0-0.5m from the simulations for both agitators. For the fermenter, the value of ε_T was calculated as 1.85 W/kg. This gave a microscale turbulence size, λ_k, of 1.44×10^{-4} m (143μm). Comparing this with the diameter of a yeast cell, which ranges between 5-10μm, the eddy current magnitude is significantly larger. The mathematical logic presented by Kolmogorov, 1941, highlights that when the turbulences are of a magnitude greater than that of the dimensions of the impacted contents, then no damage occurs to them (Kolmogorov, 1941). So, in the case of the yeast cells in question, they will partake in the turbulence in their entirety, as opposed to be impacted upon by it, as the turbulence carries it in its full due to its greater magnitude. Hence it can be concluded that the assessed power dissipation and agitation speeds simulated will not cause notable damage to the cells as a result of eddy currents.

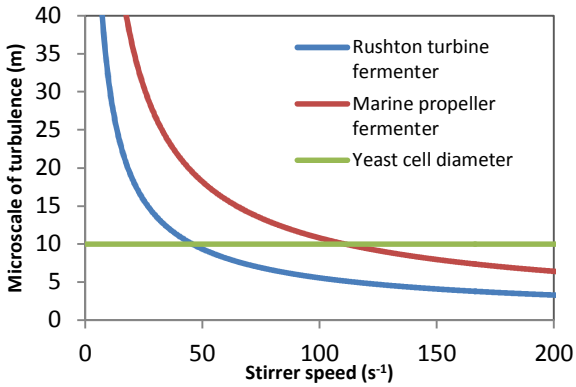

Figure 2: The decline in eddy turbulence lengths with

increase in stirrer speed. The intersection between the eddy turbulence length for Rushton (blue) and Marine (red) agitated vessels with the upper limit of the *S. cerevisiae* cell diameter range (green) is shown.

Fig. 2 presents the size of eddy turbulences created by the Rushton agitated vessel (blue) and the Marine agitated (red) with an increase in agitation stirrer speed. The upper limit of the yeast cell diameter range for *S. cerevisiae* (green); 10µm; intersects the agitation turbulence lengths at approximately $45s^{-1}$, meaning operating at such a stirring speed would generate turbulences of the same magnitude as the cell size and thus result in shear damage. From Eq. 4, the critical agitation stirring speed n_C was found to be $1.31s^{-1}$ and $0.27s^{-1}$ for the Rushton turbine and the Marine propeller respectively. Hence, agitation speeds operated at a much larger value, enough to result in shear damage as modelled in Fig.2 would not be practical, and thus eddy turbulences are unlikely to have a negative impact on operation for either agitated vessels.

4.5 Further comparisons & cost optimisation

Comparing the power consumption, and therefore operating cost, of the two agitators, Fig. 3 indicates that the Marine propeller requires much less power in order to operate at the same stirring speeds as the Rushton turbine, beyond $1s^{-1}$. Given that the Rushton turbine must be operated at an agitation speed of $1.31s^{-1}$ in order to keep all yeast cells in suspension, whereas the Marine propeller achieves full suspension at a much lower agitation of 0.27s-1, the Marine propeller is the more efficient choice from both an energy consumption and cost effective point of view.

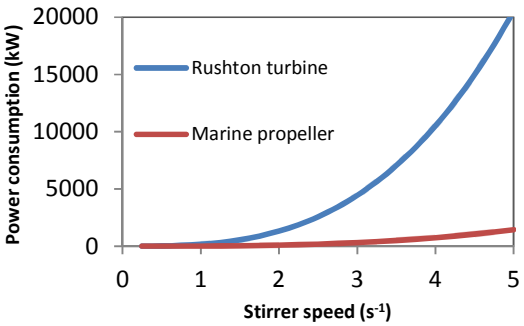

Figure 3: Power consumption within typical stirring speed range for Rushton turbine and Marine propeller.

5. Conclusions

In conclusion, modelling and running COMSOL simulations of the two differently agitated vessels proved to be useful for assessing a variety of physical parameters for batch vessel mixing; fluid vector patterns and flow, streamline flow patterns, energy dissipation resulting in shear damage to yeast cells, and enabled the designing of further properties such as suitable agitation power consumption, critical stirring velocities for cell suspension, and ultimately, selection of the most efficient agitator of the two. From a process perspective, both agitators are suitable in achieving desirable mixing within the vessels, however, from an energy and cost perspective, the Marine propeller was found to be most suitable for the modelled bioethanol fermentation processes that employ *S. cerevisiae*.

6. References

1. Doran, P., Bioprocess Engineering Principles. London: Academic Press Ltd. (1995).

2. Fogler, H. S., Elements of Chemical Reaction Engineering. 4th ed. Westford, Massachusetts: Pearson Education (2006).

3. Kolmogorov, A. N., The local structure of turbulence in incompressible viscous fluid for very large Reynolds numbers. *Dokl Akad Nauk SSSR [Translated from Russian]*, **434**, pp. 9-13 (1941).

4. McCabe, W. L., et al., Unit Operations of Chemical Engineering. 5th ed. Singapore: McGraw-Hill (1993).

5. Nienow, A. W., Stirred Tank Bioreactors: *Advanced Biochemical Engineering*, **1** (2014).

6. Riet, V., Reviewing of measuring method and results in nonviscous gas-liquid mass transfer in stirred vessels. *Industrial Engineering Chemistry Product Research*, **18**, pp. 357-364 (1979).

7. Rushton, J. H., et al., Power characteristics of mixing impellers. *Chemical Engineering Progress*, **46**, pp. 467-476 (1950).

8. Sinnott, R. K., Coulson & Richardson's:

Chemical Engineering Design. 4th ed. Oxford: Elsevier Butterworth Heinemann (2005).

7. Acknowledgements

The author would like to thank the members of her family for their continued support in her research and projects. She would further like to extend her thanks to Dr G. Vladisavljevic, senior lecturer at Loughborough University, UK, for his supervision and guidance throughout this research.

8. Appendices

MATLAB/Polymath coding, simulation raw data, simulation files, calculations/spreadsheets and mechanical drawings and data sheets can be provided upon request for researchers who wish to benefit. The author can be contacted as per email address given above.

8.1 Rushton's correlation

Fig.4 indicates that a *Re* value greater than 10^4 is a system operating in turbulent flow.

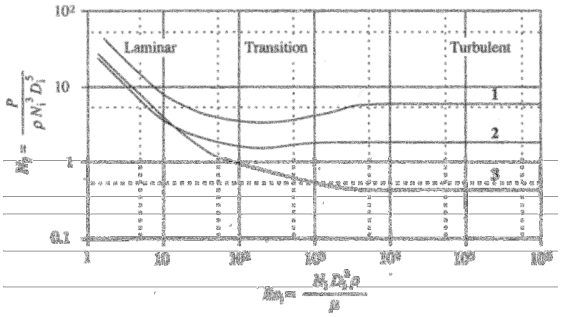

Figure 4: Correlation between Reynold's number and power number (Rushton, 1950).

8.2 Further Simulation Modelling

Height of vessels

$$H = C + \frac{V - \frac{1}{2}\left(\frac{4}{3}\,\pi\, C \left(\frac{T}{2}\right)^2\right)}{\pi\left(\frac{T}{2}\right)^2} \qquad \text{Eq. 12}$$

Vessel wall thickness

The wall thickness, *e*, of the batch reactor vessels can be found using Eq. 13 (Sinnott, 2005), where *Pi* is the internal vessel pressure, *T* is the operating temperature, *f* is the design stress of the material.

$$e = \frac{P_i T}{2f - P_i} \qquad \text{Eq. 13}$$

Ellipsoidal head design

Eq.14 (Sinnott, 2005) permits the design of the ellipsoidal shaped vessel head wall thickness, based on design stress, vessel pressure and temperature.

$$e = \frac{P_i T}{2fJ + 0.2P_i} \qquad \text{Eq. 14}$$

Material design

Material	Design stress at temperature °C (N/mm²)	
	100°C	150°C
316SS	150	135

Figure 5: Material design stresses for 316SS (stainless steel) for 100°C and 150°C. The required design stress, for any temperature within this typical range, can be obtained by numerical interpolation.

8.3 Mechanical Drawing

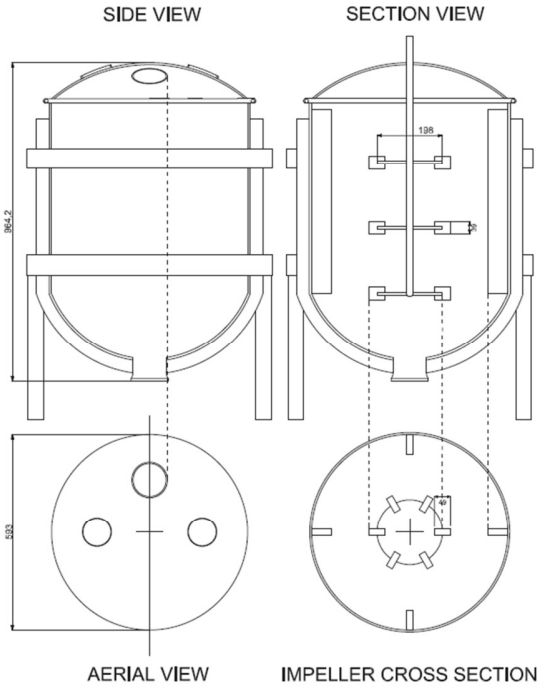

Figure 6: Mechanical 2D drawings for vessel with side view, section view, aerial view and impeller cross section (Rushton shown).